PHYSICAL REVIEW D **95,** 115032 (2017)

Dark photon relic dark matter production through the dark axion portal

Kunio Kaneta,[1] Hye-Sung Lee,[1] and Seokhoon Yun[1,2]
[1]*Center for Theoretical Physics of the Universe, Institute for Basic Science (IBS), Daejeon 34051, Korea*
[2]*Department of Physics, KAIST, Daejeon 34141, Korea*
(Received 3 May 2017; published 27 June 2017)

We present a new mechanism to produce the dark photon (γ') in the early Universe with the help of the axion (a) using a recently proposed dark axion portal. The dark photon, a light gauge boson in the dark sector, can be relic dark matter if its lifetime is long enough. The main process we consider is a variant of the Primakoff process $fa \to f\gamma'$ mediated by a photon, which is possible with the axion–photon–dark photon coupling. The axion is thermalized in the early Universe because of the strong interaction and it can contribute to the nonthermal dark photon production through the dark axion portal coupling. It provides a two-component dark matter sector, and the relic density deficit issue of the axion dark matter can be addressed by the compensation with the dark photon. The dark photon dark matter can also address the reported 3.5 keV x-ray excess via the $\gamma' \to \gamma a$ decay.

DOI: 10.1103/PhysRevD.95.115032

I. INTRODUCTION

Conventional attitudes toward the new physics are based on the presumption that the new particles have a similar coupling size as the standard model (SM) couplings. There are many popular models leading to this, including the supersymmetry, extra dimension, and grand unified theories. In this approach, after one energy scale is probed at some level, it is essential to increase the energy of the experiments to find a new uncovered particle, which typically means building a larger, higher energy beam facility. Among them are the currently running 13 TeV Large Hadron Collider and an envisioned 100 TeV collider. This line of research is categorized as the energy frontier [1].

There has been an alternative attitude toward the new physics, which is perhaps less popular yet long-standing. The new particles may have a significantly smaller coupling, at least to the SM particles, which makes them hard to detect in the typical experiments designed to probe particles of an ordinary-size coupling. Therefore they can be very light, and getting a higher energy may not be necessary to search for them. It is more important to have enough statistics (and even to develop new search schemes), which is called the intensity frontier [2].

General attitudes towards the new particles also affect the cosmic frontier [3], including the dark matter search. The typical weakly interacting massive particle (WIMP) search using nuclear recoil assumes a weak-scale new particle for dark matter [4–7]. Yet there are very light (say, below GeV scale) dark matter candidates which require completely different search schemes.

Axions (spin-0 light pseudoscalars) and dark photons (spin-1 light vector bosons) are two popular candidates of the light, feebly interacting new particles. Depending on their mass and coupling, each can be a dark matter candidate. Although less popular than the WIMP dark matter candidate, each of the two has its own history of many theoretical and experimental investigations.

Recently, it was pointed out that a genuinely new coupling $G_{a\gamma\gamma'}$ that combines the axion (a) and dark photon (γ') is possible [8]. Introduction of this coupling inevitably brings a $G_{a\gamma'\gamma'}$ coupling too. They are collectively named the "dark axion portal" [8]. (In some sense, the $G_{a\gamma'\gamma'}$ coupling was first studied in the mirror world models in which a massless mirror photon couples to the axion [9,10]. See also a recent study in the cosmological relaxation mechanism for a solution to the hierarchy problem [11].) The dark axion portal couplings can be as large as the typical axion coupling $G_{a\gamma\gamma}$ or even larger depending on the model.

As both the axion and dark photon can be dark matter candidates, the new portal is important because it makes a connection between the two dark matter candidates. In Ref. [8], a specific model called the "dark KSVZ model" was presented to realize the dark axion portal and an illustration was made of how the dark photon can be produced in the early Universe using the $G_{a\gamma'\gamma'}$ coupling. The dark photon dark matter produced with the help of the axion can compensate the deficit relic density, which is a long-standing problem of axion dark matter for $f_a \gtrsim 10^{11}$ GeV, where f_a is the Peccei-Quinn (PQ) symmetry breaking scale.

In this paper, we mainly exploit the other coupling $G_{a\gamma\gamma'}$ and investigate a new dark photon production scenario in the early Universe. With a new coupling, a novel dark photon production channel $fa \to f\gamma'$ is possible. It is similar to the Primakoff process using the $G_{a\gamma\gamma}$ coupling, and we call it the "dark Primakoff" process. Interestingly, this coupling allows the $\gamma' \to \gamma a$ decay that can address the reported 3.5 keV x-ray excess [12–17]. We will also

elaborate on the $G_{a\gamma'\gamma'}$ process by providing a more detailed description compared to the brief illustration in Ref. [8].

The rest of this paper is organized as follows. In Secs. II and III, we give brief overviews on the axion and dark photon physics, respectively. In Sec. IV, we discuss the dark axion portal and benchmark points that we want to study in this paper. In Sec. V, we investigate the dark photon production in the early Universe using the dark axion portal couplings $G_{a\gamma\gamma'}$ and $G_{a\gamma'\gamma'}$. In Sec. VI, we address the 3.5 keV x-ray excess from the dark photon decay. We devote Sec. VII to discussions on some issues. We summarize our results in Sec. VIII.

II. OVERVIEW OF PECCEI-QUINN SYMMETRY AND AXION MODELS

The strong CP problem is one of the long-standing issues in particle physics. Once we introduce the vacuum angle $\bar{\theta}_s$ as $\bar{\theta}_s G_{\mu\nu}\tilde{G}^{\mu\nu}$, we encounter the CP violation in QCD. From the experimental side, the measurement of the neutron dipole moment gives a stringent constraint, $\bar{\theta}_s \lesssim 10^{-10}$ [18], while from the theoretical side, no reason exists to keep its value that small as $\bar{\theta}_s \sim \mathcal{O}(1)$ is naturally expected. One of the promising solutions for the strong CP problem is the global PQ symmetry [19,20], the breaking of which gives rise to the QCD axion, a pseudo-Nambu-Goldstone boson, that makes the $\bar{\theta}_s$ vanish dynamically.

In the original axion models [19–22], the $U(1)_{\rm PQ}$ symmetry is supposed to be spontaneously broken down at the electroweak scale, $v_{\rm EW}$, and the massless axion emerges. The nonperturbative QCD effect explicitly violates the PQ symmetry, and the axion potential is lifted up, allowing the axion to acquire finite mass of the order of $\Lambda_{\rm QCD}^2/v_{\rm EW}$, with $\Lambda_{\rm QCD}$ being the confinement scale. On the other hand, due to the relatively large coupling among the axion and the SM particles, this $\mathcal{O}(100\ {\rm keV})$ axion model has been excluded by the rare decay measurements of mesons [23].

The invisible axion models were then proposed to evade various experimental constrains. The Kim-Shifman-Vainshtein-Zakharov (KSVZ) [24,25] and Dine-Fischler-Srednicki-Zhitnitsky (DFSZ) [26] axion models are known as viable realizations. Their main idea is to raise the breaking scale of the $U(1)_{\rm PQ}$, much larger than the electroweak scale, $f_a \gg v_{\rm EW}$, by introducing new particles that make the axion interactions feeble as they are proportional to $1/f_a$.

Although the invisible axion still suffers from astrophysical constraints with $f_a \lesssim 10^9$ GeV, it has great merit for dark matter physics; i.e., the coherent oscillation of the axion can constitute the dark matter in the Universe. When the PQ symmetry breaking takes place in the early Universe, the axion field value is randomly distributed along the degenerated vacuum with the angle $\theta_i = a_{\rm ini}/f_a$, in which $a_{\rm ini}$ is the initial field value of the axion. After the QCD phase transition occurs, the axion starts to oscillate at the time when the cosmic expansion becomes slow compared to the oscillation frequency, and thus the energy density of this oscillation plays the role of the cold dark matter (CDM) [27–29]. This scenario is called the misalignment mechanism, and the resultant CDM abundance is given by

$$\Omega_a h^2 \simeq 0.12 \times \left(\frac{f_a}{5.4\times 10^{11}\ {\rm GeV}}\right)^{1.19} \theta_i^2 F(\theta_i), \quad (1)$$

where the anharmonic effect in the axion potential is taken into account by the $F(\theta_i)$ [30]. It should be noted that for $\theta_i \lesssim 1$ the anharmonic effect is negligible, and we can take $F(\theta_i) \sim 1$; otherwise $F(\theta_i)$ gets monotonically increasing up to a factor of a few. To evade the overproduction of the axion CDM, we need $f_a \lesssim 10^{12}$ GeV for $\theta_i = \mathcal{O}(1)$.

III. OVERVIEW OF VECTOR PORTAL AND DARK PHOTON

A gauge boson much lighter than the electroweak scale can be constructed in various scenarios [31–33]. It has decades of history (for instance, see Ref. [34]) with different names. A light gauge boson physics has motivations from the dark-matter-related phenomena (such as the explanation of the positron excess [35] and self-interacting dark matter [36]) as well as non-dark-matter-related phenomena (such as the muon anomalous magnetic moment anomaly [37–39]).

For such a light gauge boson to survive all the experimental constraints, it should have a very small coupling to the SM fermions. Typically a dark gauge symmetry $U(1)_{\rm Dark}$ is assumed under which the SM fermions do not carry a charge, and its gauge boson couples to the SM fermions only through a small mixing with the SM gauge boson [40]. The kinetic mixing of the $U(1)_{\rm Dark}$ with the SM $U(1)_Y$ is described by the parameter ε:

$$\mathcal{L}_{\rm kinetic} = -\frac{1}{4}B_{\mu\nu}B^{\mu\nu} + \frac{\varepsilon}{2\cos\theta_W}B_{\mu\nu}Z'^{\mu\nu} - \frac{1}{4}Z'_{\mu\nu}Z'^{\mu\nu}. \quad (2)$$

For a light Z', the interaction Lagrangian of the physical Z' is given by [41]

$$\mathcal{L}_{\rm int} \simeq -\varepsilon e J^{\mu}_{\rm EM} Z'_{\mu} - \varepsilon \tan\theta_W \frac{m_{Z'}^2}{m_Z^2} g_Z J^{\mu}_{\rm NC} Z'_{\mu}, \quad (3)$$

where e and g_Z are the electromagnetic coupling and weak neutral current coupling ($g_Z = g/\cos\theta_W$), respectively. $J_{\rm EM}$ ($J_{\rm NC}$) is the electromagnetic (weak neutral) current. Equation (3) suggests that we can ignore its coupling to the weak neutral current as long as the ratio $m_{Z'}/m_Z$ is sufficiently small, and this is the limit we take in this

paper. As it couples predominantly to the electromagnetic current, it is typically called the dark photon.

We note that the specific form of the coupling to the weak neutral current in Eq. (3) depends on the mechanism of how the Z' gets a mass. For instance, if the Higgs sector is based on the two-Higgs-doublet model, a light Z' may still have a sizable coupling to the weak neutral current as shown in the dark Z model [43]. (In these models, a charged Higgs is introduced whose major decay mode can be strikingly different due to the light gauge boson [44–47].) We will consider more general cases including the case in which the neutral current contribution is important in a future work.

IV. DARK AXION PORTAL

Now let us consider the framework in which the axion and dark photon coexist. The axion portal to the SM gauge fields is given by

$$\mathcal{L}_{\text{axion portal}} = \frac{G_{agg}}{4} a G_{\mu\nu}\tilde{G}^{\mu\nu} + \frac{G_{a\gamma\gamma}}{4} a F_{\mu\nu}\tilde{F}^{\mu\nu} + \cdots, \quad (4)$$

where $G_{\mu\nu}$ and $F_{\mu\nu}$ are the field strength of the gluon and photon, respectively, and the tilde represents the dual of the field strength. In addition, a new portal coupling, the dark axion portal [8], can emerge by introducing the dark photon, which is given by

$$\mathcal{L}_{\text{dark axion portal}} = \frac{G_{a\gamma'\gamma'}}{4} a Z'_{\mu\nu}\tilde{Z}'^{\mu\nu} + \frac{G_{a\gamma\gamma'}}{2} a F_{\mu\nu}\tilde{Z}'^{\mu\nu}, \quad (5)$$

where $F_{\mu\nu}$ ($Z'_{\mu\nu}$) is the field strength of the photon (dark photon). Hereafter we denote the dark photon as γ' in the basis obtained by eliminating the kinetic mixing.

A simple realization of the dark axion portal is the dark KSVZ model considered in Ref. [8]. The new fields and their charges in this model are described in Table I, where ψ and ψ^c are introduced as vectorlike colored fermions, and Φ_{PQ} and Φ_D are singlet scalar fields which spontaneously break the $U(1)_{\text{PQ}}$ and $U(1)_{\text{Dark}}$ by developing a nonzero vacuum expectation value, respectively. Throughout this paper, we discuss dark matter production and relevant phenomenology by taking this setup as an example. Above the QCD scale, both the axion and dark axion portals are given by

TABLE I. New fields and their charge assignments in the dark KSVZ model. Q_ψ (D_ψ) is the electromagnetic (dark) charge of the exotic colored fermion ψ.

Field	$SU(3)_C$	$SU(2)_L$	$U(1)_Y$	$U(1)_{\text{Dark}}$	$U(1)_{\text{PQ}}$
ψ	3	1	Q_ψ	D_ψ	PQ_ψ
ψ^c	$\bar{3}$	1	$-Q_\psi$	$-D_\psi$	PQ_{ψ^c}
Φ_{PQ}	1	1	0	0	PQ_Φ
Φ_D	1	1	0	D_Φ	0

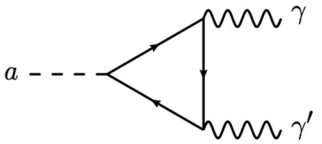

FIG. 1. The dark Primakoff mechanism is delivered by the dark axion portal coupling $G_{a\gamma\gamma'}$. The fermions inside the loop need to be charged under all $U(1)_{\text{PQ}}$, $U(1)_{\text{EM}}$, and $U(1)_{\text{Dark}}$.

$$G_{agg} = \frac{g_S^2}{8\pi^2}\frac{PQ_\Phi}{f_a}, \quad (6)$$

$$G_{a\gamma\gamma} = \frac{e^2}{8\pi^2}\frac{PQ_\Phi}{f_a}[2N_C Q_\psi^2], \quad (7)$$

$$G_{a\gamma\gamma'} = \frac{ee'}{8\pi^2}\frac{PQ_\Phi}{f_a}[2N_C D_\psi Q_\psi] + \varepsilon G_{a\gamma\gamma}, \quad (8)$$

$$G_{a\gamma'\gamma'} = \frac{e'^2}{8\pi^2}\frac{PQ_\Phi}{f_a}[2N_C D_\psi^2] + 2\varepsilon G_{a\gamma\gamma'}, \quad (9)$$

at the leading order with respect to ε, where $N_C = 3$ is the color factor, g_S is the $SU(3)_C$ gauge coupling, and e' is the $U(1)_{\text{Dark}}$ gauge coupling. Here, we define $f_a^2 = 2PQ_\Phi^2\langle\Phi_{PQ}\rangle^2$ and in the following discussion we will take $PQ_\Phi = -(PQ_\psi + PQ_{\psi^c}) = 1$ for the purpose of illustration.

We emphasize that the dark axion portal (in other words, vector-axion portal) is not a product of two other portals (the vector portal and axion portal). The second terms in Eqs. (8) and (9) are from that product, but the first terms are not. The first terms originate from the exotic fermions in the triangle loop that couple to the axion, photon, and dark photon directly (see Fig. 1).

In the next section, we will study the following two cases as the benchmark scenarios,

Case (i): $Q_\psi = 0$ and $D_\psi = 3$,

Case (ii): $Q_\psi = -1/3$ and $D_\psi = 3$.

For definiteness we will assume $\varepsilon \simeq 0$. The axion and dark axion portal couplings in these cases are given in Table II.

Before closing this section, let us comment on taking the vanishing kinetic mixing. This is possible because the ε is a free parameter at the tree level. On the other hand, this parameter choice does not hold if there is a radiatively induced kinetic mixing. For instance, in the case (ii), since the exotic fermion is charged under both $U(1)_{\text{EM}}$ and

TABLE II. The relevant axion portal couplings and dark axion portal couplings. For all terms, a common factor $\frac{1}{8\pi^2}\frac{PQ_\Phi}{f_a}$ is omitted.

Case	G_{agg}	$G_{a\gamma\gamma}$	$G_{a\gamma\gamma'}$	$G_{a\gamma'\gamma'}$
(i) $Q_\psi = 0$, $D_\psi = 3$	g_S^2	0	0	$e'^2(54)$
(ii) $Q_\psi = -\frac{1}{3}$, $D_\psi = 3$	g_S^2	$e^2(2/3)$	$ee'(-6)$	$e'^2(54)$

$U(1)_{\rm Dark}$, the mixing between γ and γ' is induced at the one-loop level. The order of magnitude of the induced kinetic mixing is estimated by following the renormalization group (RG) evolution, where we define $\beta_\varepsilon \equiv d\varepsilon/d\log\mu$. For the RG scale μ above the exotic fermion mass m_ψ, we have

$$\beta_\varepsilon(\mu > m_\psi) = \frac{ee'}{6\pi^2} N_{C,\psi} Q_\psi D_\psi, \tag{10}$$

where $N_{C,\psi} = 3$ is the number of color degrees of freedom. For instance, if we take $\varepsilon = 0$ at a certain scale Λ higher than m_ψ, such as the grand unification scale, we obtain the induced value of the ε,

$$\varepsilon_{\rm induced} = \frac{ee'}{6\pi^2} N_{C,\psi} Q_\psi D_\psi \log\left(\frac{m_\psi}{\Lambda}\right), \tag{11}$$

at an energy scale lower than m_ψ. It should be noted that for $\mu < m_\psi$, the RG running of ε is given by

$$\beta_\varepsilon(\mu < m_\psi) = \varepsilon \frac{e^2}{6\pi^2} \sum_f N_{C,f} Q_f^2, \tag{12}$$

where Q_f and $N_{C,f}$ are the electric charge and color factor of the SM fermion f. Since there is an additional ε in Eq. (12), the RG running of ε below m_ψ is negligibly small.

Therefore, the radiatively induced kinetic mixing is estimated as $\varepsilon_{\rm induced} \approx 0.015 e' \log(m_\psi/\Lambda)$ for $Q_\psi D_\psi = 1$ and $\varepsilon_{\rm induced} \sim -\mathcal{O}(10^{-2})$ if we take $e' = 0.1$ with $\Lambda \sim 10^{16}$ GeV (typical GUT scale) and $m_\psi \sim f_a$ (10^9–10^{12} GeV). The induced value itself is inconsistent with astrophysical observations and the beam dump experiments for the keV-MeV scale dark photon [2].

On the other hand, the ε value at the UV scale (Λ) is not determined in general, and we can take $\varepsilon = \varepsilon(\Lambda) + \varepsilon_{\rm induced}$ sufficiently small at the cost of fine-tuning. Alternatively, it is also possible to suppress the radiatively induced ε by introducing another exotic fermion having the same mass as ψ and opposite dark charge, by which the cancellation between the contributions from these two fermions can occur [40,43]. Since our discussion is independent from the number of exotic fermions, our main result does not change as long as additional fermions do not contribute to the dark axion portal significantly.

V. DARK PHOTON PRODUCTION IN THE EARLY UNIVERSE

Now, we are ready for looking at the dark photon production in the early Universe, where the dark photon can be a good candidate for the dark matter. As the dark photon feebly couples to the SM particles due to the large f_a, it never reaches a thermal equilibrium in most parameter space; the dark photon is nonthermally produced.

We will discuss case (i) and case (ii) in order as they employ quite a different production mechanism of the dark photon (see Fig. 2). It should be noted that there is another possible production process which is not related to the dark axion portal, namely, the $gg \to \gamma'\gamma'$ process through the box diagram induced by the ψ loop. However, this process becomes negligible when the mass of ψ is heavy, such as f_a, as long as we take $T < f_a$ during the γ' production, by which the production rate of $\psi\bar{\psi} \to \gamma'\gamma'$ is naturally suppressed as well. If the reheating temperature exceeds f_a, the PQ symmetry restoration may occur, which also leads to the vanishing dark axion portal. Therefore, in the following discussion, we focus on the case where the reheating temperature does not exceed f_a so that the PQ symmetry is never restored.

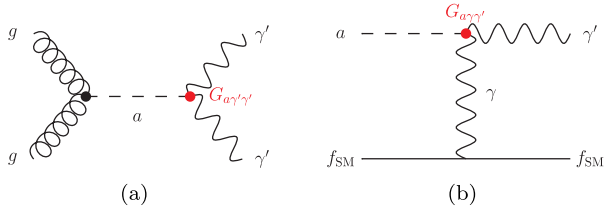

FIG. 2. New production mechanisms of the dark photon dark matter using the dark axion portal in the early Universe via (a) the axion mediation and (b) the dark Primakoff process, which is the dominant process for the case (i) $Q_\psi = 0$ and case (ii) $Q_\psi \neq 0$, respectively.

A. Case (i)

In case (i), the exotic colored fermions are electrically neutral, and the axion does not couple to the photon through the triangle diagram, which results in $G_{a\gamma\gamma} = G_{a\gamma\gamma'} = 0$. Since $G_{a\gamma'\gamma'}$ is only the nonvanishing dark axion portal term, the dark photon can be produced via $gg \to a \to \gamma'\gamma'$ and becomes stable [Fig. 2(a)].

In Ref. [8], the freeze-in mechanism [48] for the dark photon production via $gg \to a \to \gamma'\gamma'$ is analyzed. The Boltzmann equation for the γ' is given by

$$-sHT\frac{dY_{\gamma'}}{dT} = \gamma[n_{\gamma'}], \tag{13}$$

where $Y_{\gamma'} = n_{\gamma'}/s$ is the comoving number density of the γ', $\gamma[n_{\gamma'}]$ denotes the collision term, $s = (2\pi^2/45) g_{*s} T^3$, $H^2 = (\pi^2/90) g_{*\rho} T^4/M_{\rm Pl}^2$ with $M_{\rm Pl} \simeq 2.4 \times 10^{18}$ GeV, and $g_{*s} = g_{*\rho} \equiv g_*$ is taken as a constant value in our analysis. The annihilation cross section of this process is $\sigma v \simeq 4 G_{agg} G_{a\gamma'\gamma'} |A(\tau_\psi)|^2 S$ with $A \equiv A(\tau_\psi)$ being the loop function given by

$$A(\tau_\psi) = \frac{1}{\tau_\psi} \begin{cases} \arcsin^2\sqrt{\tau_\psi} & \tau_\psi \le 1 \\ -\frac{1}{4}\left[\log\frac{1+\sqrt{1-\tau_\psi^{-1}}}{1-\sqrt{1-\tau_\psi^{-1}}} - i\pi\right]^2 & \tau_\psi > 1, \end{cases} \tag{14}$$

where $\tau_\psi \equiv S/(4m_\psi^2)$, with m_ψ and S being the mass of ψ and the squared collision energy, respectively. In the case that the ψ is very heavy compared to the reheating temperature, we can take $A(\tau_\psi) \simeq 1$ in the thermally averaged cross section, and hereafter we restrict ourselves to this heavy ψ case. Then, the collision term in Eq. (13) is given by

$$\gamma_{gg\to\gamma'\gamma'} \simeq \frac{48}{\pi^4} G_{agg}^2 G_{a\gamma'\gamma'}^2 T^8, \tag{15}$$

which leads to

$$\Omega_{\gamma'}h^2 \simeq 0.12 \times g_D^4 \left(\frac{100}{g_*}\right)^{3/2} \left(\frac{m_{\gamma'}}{10\ \mathrm{keV}}\right) \times \left(\frac{5T_{\mathrm{RH}}}{f_a}\right)^3 \left(\frac{10^{10}\ \mathrm{GeV}}{f_a}\right), \tag{16}$$

where $m_{\gamma'}$ and T_{RH} are the mass of the dark photon and the reheating temperature, respectively, and we define $g_D \equiv e' D_\psi/0.3$.

The observed dark matter number density is accounted for by the axion and dark photon together, $\Omega_{\mathrm{DM}}h^2 = (\Omega_{\gamma'} + \Omega_a)h^2 = 0.12$, and it is shown in Fig. 3 for $g_D = 1$. In the figure, the blue solid and dashed curves become horizontal in the large f_a region, since the whole amount of the dark matter density can be explained by the axion alone, while in the smaller f_a region the dark photon can compensate the shortage of the axion dark matter. In the case of $\Omega_{\mathrm{DM}}h^2 = \Omega_{\gamma'}h^2$, the dark photon lighter than $O(1$–$10)$ keV may affect the small-scale structure, and thus the Lyman-α forest gives a lower limit on $m_{\gamma'}$, depicted by the orange region in Fig. 3, which we take as $m_{\gamma'} \lesssim 12$ keV [49].[1] It should be noted that there is an upper bound on T_{RH}, since if T_{RH} were sufficiently high, γ' could have been thermalized and produced too much to explain the observed value. By demanding $H(T_{\mathrm{RH}}) < \gamma_{gg\to\gamma'\gamma'}(T_{\mathrm{RH}})/n_{\gamma'}^{\mathrm{eq}}(T_{\mathrm{RH}})$, with $n_{\gamma'}^{\mathrm{eq}} \simeq [3\zeta(3)/\pi^2]T^3$, we obtain

$$T_{\mathrm{RH}} \lesssim 10^{10}\ \mathrm{GeV} \times g_D^{4/3} \left(\frac{g_*}{100}\right)^{1/6} \left(\frac{f_a}{10^{10}\ \mathrm{GeV}}\right)^{4/3}, \tag{17}$$

which can be satisfied by taking a larger $m_{\gamma'}$ for the dark matter abundance to be the observed value (see Fig. 3).

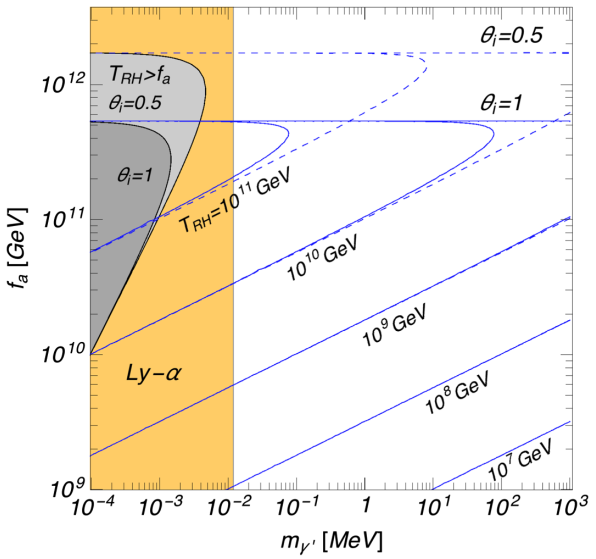

FIG. 3. The blue curves show $\Omega_{\mathrm{DM}}h^2 = (\Omega_{\gamma'} + \Omega_a)h^2 = 0.12$ for the given T_{RH} with the initial misalignment angle $\theta_i = 0.5$ (blue dashed curves) and $\theta_i = 1$ (blue solid curves) in the case (i) for a choice of $g_D = 1$. The gray regions are disfavored, since the reheating temperature to obtain the correct dark matter density exceeds f_a, restoring the PQ symmetry. The orange region shows the Lyman-α constraint only for the case of $\Omega_{\mathrm{DM}}h^2 = \Omega_{\gamma'}h^2$.

B. Case (ii)

In case (ii), since the ψ is electrically charged, the $G_{a\gamma\gamma'}$ does not vanish, which leads to the decay of the γ' into the axion and photon. The partial decay width of $\gamma' \to a\gamma$, which is the main decay channel, is given by

$$\Gamma(\gamma' \to \gamma a) = \frac{G_{a\gamma\gamma'}^2}{96\pi} m_{\gamma'}^3 \left[1 - \frac{m_a^2}{m_{\gamma'}^2}\right]^3. \tag{18}$$

For small $m_{\gamma'}$ and/or large f_a, the dark photon becomes a sufficiently long-lived particle so that it can be dark matter.

At higher temperature ($T \gg v_{\mathrm{EW}}$), the axion is also thermalized through $gg \leftrightarrow ga$ and other hadronic processes [50–52]. Therefore, the dark photon production through the dark Primakoff process, $fa \to f\gamma'$ with γ' being nonthermal, becomes efficient, which is similar to the thermal axion production in the electron-photon scattering ($\gamma e \to ae$) [53].

The $G_{a\gamma\gamma'}$ also contributes to another γ' abundance produced by the annihilation of the SM particles ($f\bar{f} \to \gamma \to a\gamma'$). Since the γ involved in this s-channel process has the thermal mass, the plasmon decay takes place if the temperature is high enough. Compared to the dark Primakoff process, however, the plasmon decay contribution is negligible [54].

It would be worthwhile to note that if there are direct couplings between γ' and the SM fermion through, for instance, the kinetic mixing, the t-channel annihilation process, $f\bar{f} \to \gamma' V$, with V being the SM gauge bosons, may also give a significant contribution at high temperature [55], which we have omitted by turning off the kinetic mixing.

[1] Although a careful analysis of the power spectrum is needed for a more accurate constraint, we have taken this crude value by maintaining the entropy density for the early-decoupled dark matter case.

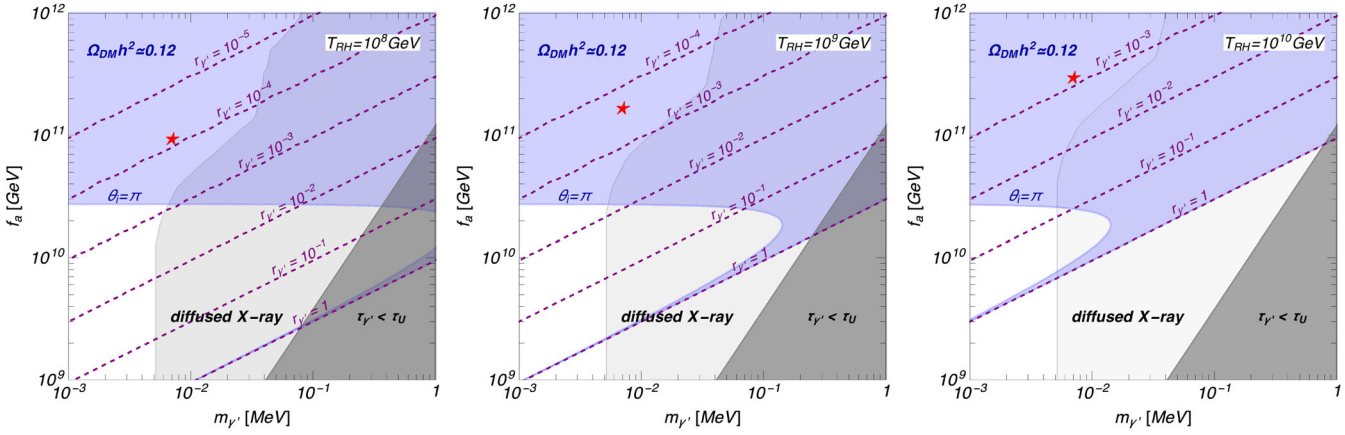

FIG. 4. The blue regions show $\Omega_{\rm DM}h^2=(\Omega_{\gamma'}+\Omega_a)h^2=0.12$ with the initial misalignment angle θ_i varying from 0 to π in the case (ii) for a choice of $\bar{g}_D=1$. It depends on the reheating temperature, and we illustrate for $T_{\rm RH}=$ (a) 10^8 GeV, (b) 10^9 GeV, and (c) 10^{10} GeV. The dark and light gray regions depict the bounds from $\tau_{\gamma'}<\tau_U$ and the observations of the diffused x-ray, respectively. The red stars indicate the points that can explain the 3.5 keV x-ray excess via the $\gamma'\to\gamma a$ decay.

The collision term of the dark Primakoff process is given by

$$\gamma_{fa\to f\gamma'}\simeq g_F(T)\frac{T^6}{\pi^4}\frac{e^2G_{a\gamma\gamma'}^2}{8\pi}\left(\log\frac{T^2}{m_\gamma^2}+\alpha_{\gamma'}\right), \quad (19)$$

where $g_F\equiv\sum_f g_f Q_f^2$ counts the number of the relativistic degrees of freedom g_f of electrically charged fermions at the temperature T, and $\alpha_{\gamma'}=3/4-2\gamma_E+\log 4$ with γ_E being Euler's constant given by $\gamma_E\simeq0.5772$. For more detail about Eq. (19), see the Appendix. Here, we have introduced the photon thermal mass $m_\gamma\sim eT$ to regulate the infrared divergence.[2] By integrating $dY_{\gamma'}/dT$ over T from $T=T_{\rm RH}$ to $T\simeq0$ in Eq. (13), we obtain

$$Y_{\gamma'}^0\simeq\frac{135\sqrt{10}}{2\pi^7 g_*^{3/2}}\frac{4e^2G_{a\gamma\gamma'}^2}{\pi}M_{\rm Pl}T_{\rm RH}\times\frac{g_F(T_{\rm RH})}{32}\left(\log\frac{T^2}{m_\gamma^2}+\alpha_{\gamma'}-2\right), \quad (20)$$

and thus the dark photon abundance is given by

$$\Omega_{\gamma'}h^2\simeq0.12\times\bar{g}_D^2\left(\frac{Q_\psi}{1/3}\right)^2\left(\frac{100}{g_*}\right)^{3/2}\left(\frac{g_F(T_{\rm RH})}{32}\right)\times\left(\frac{m_{\gamma'}}{\rm MeV}\right)\left(\frac{10^2}{f_a/T_{\rm RH}}\right)\left(\frac{10^{10}}{f_a/{\rm GeV}}\right), \quad (21)$$

[2]While this cutoff method is often used (e.g., Refs. [56,57]), a more accurate treatment exists [53]. The cutoff method, however, provides the resultant reaction rate at the same order of magnitude as that obtained by the more rigorous calculation, and this is good enough for our purpose in this paper.

with $\bar{g}_D\equiv e'D_\psi/0.01$.

In addition to the dark Primakoff process, there is another contribution from $gg\to\gamma'\gamma'$ as discussed in case (i). However, because of the difference in $\gamma_{fa\to f\gamma'}\propto1/f_a^2$ and $\gamma_{gg\to\gamma'\gamma'}\propto1/f_a^4$, the dark photon production from the dark Primakoff process is the dominant contribution in the parameter space of our interest.

Figure 4 shows the regions of $\Omega_{\rm DM}h^2=0.12$ with θ_i varying form 0 to π, for a choice of $\bar{g}_D=1$. Each panel of the figure shows a different $T_{\rm RH}$ value case. The dark gray regions in the figure represent the case that the lifetime of the dark photon, $\tau_{\gamma'}$, becomes shorter than the age of the Universe, $\tau_U\simeq13.7\times10^9$ yrs. As the dark photon decays into a photon in case (ii), the nonobservation of the dark matter signal in the diffused x-ray spectrum gives a stronger constraint on the lifetime of the dark photon. A generic constraint on the dark matter lifetime is discussed in Ref. [58] from which we have estimated the bound in our case. By taking into account the dependence on

$$r_{\gamma'}\equiv\frac{\Omega_{\gamma'}h^2}{\Omega_{\rm DM}h^2} \quad (22)$$

in the diffused x-ray flux, we show its bound as light gray regions in the figure. The point noted in the red star in the figure indicates that the dark photon can explain the 3.5 keV x-ray line excess, which we will discuss in the next section.

It should be noted that there is an upper bound on $T_{\rm RH}$ for the dark photon to remain nonthermal in a way similar to Eq. (17):

$$T_{\rm RH}\lesssim(3\times10^{11}\ {\rm GeV})\bar{g}_D^{-2}\left(\frac{g_*}{100}\right)^{1/2}\left(\frac{f_a/{\rm GeV}}{10^{10}}\right)^2. \quad (23)$$

In addition, for the dark Primakoff process to be effective, the axion should still be in a thermal bath during the dark photon production. The thermalization of the axion is maintained by the reaction $gg \leftrightarrow ga$, whose decoupling temperature T_D is given by [52]

$$T_D \simeq (10^5\ \mathrm{GeV})\left(\frac{f_a}{10^{10}\ \mathrm{GeV}}\right)^2, \tag{24}$$

and thus $T_{\mathrm{RH}} > T_D$ should be satisfied. Therefore, in the case of $\Omega_{\gamma'} \gg \Omega_a$, i.e., $\Omega_{\gamma'}h^2 \simeq 0.12$, the conditions (23) and $T_{\mathrm{RH}} > T_D$, respectively, give the lower and upper bounds on $m_{\gamma'}$, and we obtain $1\ \mathrm{keV} \lesssim m_{\gamma'} \lesssim 1\ \mathrm{GeV} \times \bar{g}_D^{-2}$. The regions realizing $\Omega_{\gamma'} \gg \Omega_a$ are, however, disfavored by the diffused x-ray bound and the requirement of $T_{\mathrm{RH}} \ll f_a$, as shown in Fig. 4.

VI. DARK PHOTON EXPLANATION OF THE 3.5 KEV X-RAY LINE EXCESS

In various x-ray observations of galaxy clusters, it has been observed that there is an anomalous excess at 3.5 keV in the x-ray spectra from galaxies [12–17], and thus it is worth discussing whether it can be explained by the dark photon dark matter in our scenario.

It is known that the dark matter mass (m_{DM}) and its lifetime (τ_{DM}) (with a decay to a photon final state) are required to be [13]

$$m_{\mathrm{DM}} \simeq 7\ \mathrm{keV}, \tag{25}$$

$$\tau_{\mathrm{DM}} \simeq 10^{28}\ \mathrm{sec} \simeq 3 \times 10^{20}\ \mathrm{yrs}, \tag{26}$$

so that the particle dark matter can explain the 3.5 keV x-ray line.[3] The case (i) does not have the dark photon decay mode to the photon while the case (ii) does. In the following discussion, we consider only the $\gamma' \to \gamma a$ in case (ii) and take $G_{a\gamma\gamma'}$ as a free parameter instead of specifying e' and Q_ψ.

In case (ii), the lifetime of the dark photon is given by

$$\tau_{\gamma'} \simeq (1.5 \times 10^{25}\ \mathrm{sec})\left(\frac{10^{-16}\ \mathrm{GeV}^{-1}}{G_{a\gamma\gamma'}}\right)^2\left(\frac{7\ \mathrm{keV}}{m_{\gamma'}}\right)^3 \tag{27}$$

from Eq. (18), which is shorter than the condition (26). On the other hand, when the dark photon is responsible for only a fraction of the total dark matter abundance, the condition changes to [62]

$$\tau_{\mathrm{DM}} \simeq r_{\gamma'} \times 10^{28}\ \mathrm{sec}, \tag{28}$$

where $r_{\gamma'}$ can be written in terms of $G_{a\gamma\gamma'}$ as

$$r_{\gamma'} \simeq 10^{-3}\left(\frac{100}{g_*}\right)^{3/2}\left(\frac{T_{\mathrm{RH}}}{10^{11}\ \mathrm{GeV}}\right) \times \left(\frac{G_{a\gamma\gamma'}}{10^{-16}\ \mathrm{GeV}^{-1}}\right)^2\left(\frac{m_{\gamma'}}{7\ \mathrm{keV}}\right), \tag{29}$$

and thus the dark photon can produce the observed 3.5 keV x-ray line if $\tau_{\gamma'}$ of Eq. (27) satisfies the condition (28).

In Fig. 5, we fix $m_{\gamma'} = 7$ keV as required by the condition (25). The red line shows the parameter region that can explain the 3.5 keV x-ray excess by satisfying the condition (28), while the gray solid lines correspond to several values of $r_{\gamma'}$. The 3.5 keV solution provides a relation between the $G_{a\gamma\gamma'}$ and T_{RH} as

$$G_{a\gamma\gamma'} \simeq (10^{-16}\ \mathrm{GeV}^{-1})\left(\frac{10^{11}\ \mathrm{GeV}}{T_{\mathrm{RH}}}\right)^{1/4} \tag{30}$$

or

$$\frac{f_a}{PQ_\Phi} \simeq (10^{12}\ \mathrm{GeV})\left|\frac{e'D_\psi}{0.01}\frac{Q_\psi}{1/3}\right|\left(\frac{T_{\mathrm{RH}}}{10^{11}\ \mathrm{GeV}}\right)^{1/4}, \tag{31}$$

which is illustrated as the T_{RH} increases in Fig. 4.

The condition $\Omega_{\mathrm{DM}}h^2 = 0.12$ holds in the whole region in the figure, except for the dark gray corner where the dark photon is overproduced ($\Omega_{\mathrm{DM}}h^2 \sim \Omega_{\gamma'}h^2 > 0.12$).

The lightly shaded regions of the parameter space, while satisfying the relic density condition, are disfavored by other considerations. The upper light gray regions (dotted-dashed boundary) for $G_{a\gamma\gamma'} \lesssim 10^{-15}\ \mathrm{GeV}^{-1}$ do not satisfy the upper limit on T_{RH} given by the PQ symmetry restoration condition ($T_{\mathrm{RH}} < f_a$). For $G_{a\gamma\gamma'} \gtrsim 10^{-15}\ \mathrm{GeV}^{-1}$, the dark photon nonthermalization condition to avoid DM overproduction of Eq. (23) engages. The lower light gray regions (dotted boundary) are disfavored, since the axion thermalization condition ($T_{\mathrm{RH}} > T_D$) is not satisfied. The θ_i dependence of all the light gray regions is because f_a is determined by θ_i when we demand $\Omega_{\mathrm{DM}}h^2 \sim \Omega_a h^2 = 0.12$ in the region of $r_{\gamma'} \ll 1$.

VII. DISCUSSIONS ON SOME ISSUES

In this section, we have brief discussions on several issues of the dark axion portal although they are not our main focus in this paper.

First, we discuss the direct detection of the dark photon dark matter. The axion relic dark matter is searched for using the $G_{a\gamma\gamma}$ coupling [63,64]. Assuming the dark photon dark matter makes up a large fraction of the total dark matter relic density, we briefly comment on its detection possibility. If the kinetic mixing ε is large enough, the

[3] Although the tension between such a light dark matter and the constraint from the small-scale structure is currently under debate, the tension is ameliorated if the 7 keV dark matter is a subdominant component of the whole dark matter abundance [49,59–61], which is the case we discuss.

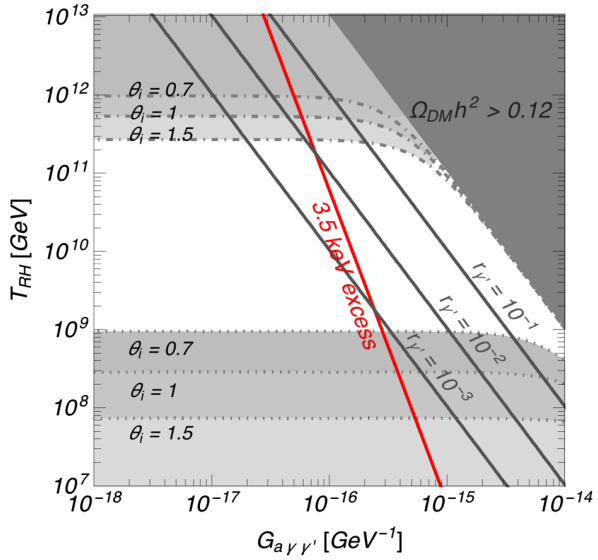

FIG. 5. Parameter space of the two-component dark matter scenario where the axion CDM is dominant and the 7 keV dark photon produced by the dark Primakoff mechanism is subdominant (with a fraction of $r_{\gamma'}$). The red line can explain the 3.5 keV x-ray line signal. The shaded regions are constrained by the PQ symmetry restoration condition (dotted-dashed bounds), the overproduction of the dark photon dark matter (dark gray corner), and the axion thermalization condition (dotted bounds). θ_i is the initial misalignment angle on which the axion relic density depends.

axion dark matter experiments [63,64] may be used to search for a dark photon dark matter of a similar mass ($m_{\gamma'} \approx 10^{-6} - 10^{-4}$ eV) [65]. When we ignore the kinetic mixing effect and consider only the $G_{a\gamma\gamma'}$ coupling, the dark photon may be searched for using a scattering with an electron inside the detector. The scattering would be mediated by the photon and the dark photon would convert into an axion, which would escape the detector. A low-Q^2 electron recoil would be a signal of such a dark photon dark matter using the dark axion portal. It would require a careful analysis to see if an existing dark matter detection experiment can detect it or if a new detector design is necessary.

Now, we recall the stability issue of the exotic quark (ψ, ψ^c). The exotic quark in the original KSVZ model does not decay at all, but it may decay in the dark KSVZ model depending on the charge assignment because of an additional particle Φ_D. For instance, the $\Phi_D^\dagger \psi D^c$ term is allowed for $PQ_\psi = 0$, $Q_\psi = -1/3$, $D_\psi = D_\Phi$ in the case (ii), which would allow the exotic quark decay into the S_D (CP-even component of the Φ_D) and a down-type quark [8]. This term might cause a flavor-changing neutral current such as $b \to s + \gamma'$, but it will be highly suppressed by the large mass of the exotic quark. In the case (i), we do not have such a decay mode, yet we can adopt the same attitude to this issue as the original KSVZ model. As the exotic quark mass scale ($f_a \gtrsim 10^9$ GeV) is larger than the reheating temperature, too few exotic quarks would have been produced in the early Universe to cause any conflict with the experimental data.

Finally, let us comment on a possible extension of the model and its phenomenology. Though we have limited ourselves to the conventional QCD axion case in this paper, where $m_a \sim (10^{-5}$–$10^{-2})$ eV and $G_{a\gamma\gamma} \sim (10^{-11}$–$10^{-14})$ GeV^{-1}, our discussion can be extended to a rather wide class of models with an axionlike particle (ALP) whose mass and coupling can be significantly larger than the QCD axion. In such models, various types of experiments can be used to test the dark axion portal, perhaps in a similar way as the colliders give constraints on the axion–photon–Z boson coupling by measuring $Z \to 3\gamma$ following $Z \to \gamma +$ ALP for a MeV-GeV scale ALP [66,67]. For instance, a monophoton signal from $Z \to \gamma + 2\gamma'$ followed by $Z \to \gamma +$ ALP and $gg \to$ ALP $\to \gamma\gamma'$ would be possible. Using the similar diagrams, a mono-Z signal would also be possible. As other interesting channels, $Z \to 2\gamma + \gamma'$ induced by the exotic fermion loop and/or followed by ALP $\to \gamma + \gamma'$ might also be worthwhile to study in the future.

VIII. SUMMARY

In this paper we have discussed a new mechanism to produce the dark photon in the early Universe with the help of the axion using the dark axion portal. In particular, the dark photon can be a dark matter candidate if its lifetime is long enough.

Our discussion is categorized into two cases based on the dark KSVZ model: (i) the vectorlike fermion is electrically neutral and (ii) it is electrically charged. In both cases the dark photon can have a longer lifetime than the age of the Universe. On the other hand, the dark photon production process is quite different in each case, while the dark photon is always a nonthermal relic due to a feeble coupling to the SM particles. In case (i), $gg \to a \to \gamma'\gamma'$ via $G_{a\gamma'\gamma'}$ is the only possible way to produce the dark photon unless we count on the kinetic mixing. Interestingly, even in the small f_a regions where the axion abundance is sufficiently small, the dark photon can compensate the dark matter abundance to achieve the observed value. The dark Primakoff process, $fa \to f\gamma'$ via $G_{a\gamma\gamma'}$, is open in case (ii) to produce the dark photon. Since the dark photon decays into a photon in this case, we have discussed the diffused x-ray constraint. It can also explain the 3.5 keV x-ray line excess as we discussed.

ACKNOWLEDGMENTS

This work was supported by Institute for Basic Science (Project Code IBS-R018-D1). H. L. appreciates the hospitality during his visit to KIAS. We thank many people,

including K. J. Bae, E. J. Chun, and P. Ko for intriguing discussions and A. Kamada for helpful comments.

APPENDIX: COLLISION TERM OF THE DARK PRIMAKOFF PROCESS

Here we give more detailed expressions related to the collision term of the dark Primakoff process in Eq. (19). Let us consider the process $fa \to f\gamma'$ by exchanging a single photon, where f denotes a SM fermion having electric charge Q_f. The squared amplitude after summing over the spin is then given by

$$|\mathcal{M}_f|^2 \simeq \frac{e^2 Q_f^2 G_{a\gamma\gamma'}^2}{2} \frac{(-T^3 - 2S^2T - 2ST^2)}{(T - m_\gamma^2)^2}, \quad \text{(A1)}$$

where S and T are the Mandelstam variables, and $m_{\gamma'} \sim eT$ is the plasmon mass. We have taken all the external particles to be massless. The collision term in the Boltzmann equation can be written as

$$\gamma_{fa\to f\gamma'} = \sum_f g_f \frac{T}{32\pi^4} \int dS(\sigma_f v) S^{3/2} K_1\left(\frac{\sqrt{S}}{T}\right), \quad \text{(A2)}$$

where g_f is the number of degrees of freedom of particle f, the cross section is given by

$$\sigma_f v \simeq \frac{e^2 Q_f^2 G_{a\gamma\gamma'}^2}{32\pi} \left(4 \log \frac{S}{m_\gamma^2} - 7\right), \quad \text{(A3)}$$

and thus we end up with

$$\gamma_{fa\to f\gamma'} \simeq g_F(T) \frac{T^6}{\pi^4} \frac{e^2 G_{a\gamma\gamma'}^2}{8\pi} \left(\log \frac{T^2}{m_\gamma^2} + \alpha_{\gamma'}\right), \quad \text{(A4)}$$

with $g_F(T) \equiv \sum_f g_f Q_f^2$ at the relevant temperature and $\alpha_{\gamma'} = 3/4 - 2\gamma_E + \log 4$.

[1] Y. Gershtein *et al.*, arXiv:1311.0299.
[2] R. Essig *et al.*, arXiv:1311.0029.
[3] A. Kusenko and L. J. Rosenberg, arXiv:1310.8642.
[4] P. Cushman *et al.*, arXiv:1310.8327.
[5] A. Tan *et al.* (PandaX-II Collaboration), Phys. Rev. Lett. **117**, 121303 (2016).
[6] D. S. Akerib *et al.* (LUX Collaboration), Phys. Rev. Lett. **118**, 021303 (2017).
[7] J. Alexander *et al.*, arXiv:1608.08632.
[8] K. Kaneta, H. S. Lee, and S. Yun, Phys. Rev. Lett. **118**, 101802 (2017).
[9] Z. Berezhiani, L. Gianfagna, and M. Giannotti, Phys. Lett. B **500**, 286 (2001).
[10] D. Ejlli, arXiv:1609.06623.
[11] K. Choi, H. Kim, and T. Sekiguchi, Phys. Rev. D **95**, 075008 (2017).
[12] E. Bulbul, M. Markevitch, A. Foster, R. K. Smith, M. Loewenstein, and S. W. Randall, Astrophys. J. **789**, 13 (2014).
[13] A. Boyarsky, O. Ruchayskiy, D. Iakubovskyi, and J. Franse, Phys. Rev. Lett. **113**, 251301 (2014).
[14] S. Riemer-Srensen, Astron. Astrophys. **590**, A71 (2016).
[15] T. E. Jeltema and S. Profumo, Mon. Not. R. Astron. Soc. **450**, 2143 (2015).
[16] A. Boyarsky, J. Franse, D. Iakubovskyi, and O. Ruchayskiy, Phys. Rev. Lett. **115**, 161301 (2015).
[17] D. Iakubovskyi, E. Bulbul, A. R. Foster, D. Savchenko, and V. Sadova, arXiv:1508.05186.
[18] C. A. Baker *et al.*, Phys. Rev. Lett. **97**, 131801 (2006).
[19] R. D. Peccei and H. R. Quinn, Phys. Rev. Lett. **38**, 1440 (1977).
[20] R. D. Peccei and H. R. Quinn, Phys. Rev. D **16**, 1791 (1977).
[21] S. Weinberg, Phys. Rev. Lett. **40**, 223 (1978).
[22] F. Wilczek, Phys. Rev. Lett. **40**, 279 (1978).
[23] W. A. Bardeen, R. D. Peccei, and T. Yanagida, Nucl. Phys. **B279**, 401 (1987).
[24] J. E. Kim, Phys. Rev. Lett. **43**, 103 (1979).
[25] M. A. Shifman, A. I. Vainshtein, and V. I. Zakharov, Nucl. Phys. **B166**, 493 (1980).
[26] M. Dine, W. Fischler, and M. Srednicki, Phys. Lett. **104B**, 199 (1981).
[27] J. Preskill, M. B. Wise, and F. Wilczek, Phys. Lett. **120B**, 127 (1983).
[28] L. F. Abbott and P. Sikivie, Phys. Lett. **120B**, 133 (1983).
[29] M. Dine and W. Fischler, Phys. Lett. **120B**, 137 (1983).
[30] K. J. Bae, J. H. Huh, and J. E. Kim, J. Cosmol. Astropart. Phys. 09 (2008) 005.
[31] N. Arkani-Hamed and N. Weiner, J. High Energy Phys. 12 (2008) 104.
[32] C. Cheung, J. T. Ruderman, L. T. Wang, and I. Yavin, Phys. Rev. D **80**, 035008 (2009).
[33] H. S. Lee and M. S. Seo, Phys. Lett. B **767**, 69 (2017).
[34] P. Fayet, Nucl. Phys. **B187**, 184 (1981).
[35] N. Arkani-Hamed, D. P. Finkbeiner, T. R. Slatyer, and N. Weiner, Phys. Rev. D **79**, 015014 (2009).
[36] S. Tulin, H. B. Yu, and K. M. Zurek, Phys. Rev. Lett. **110**, 111301 (2013).
[37] S. N. Gninenko and N. V. Krasnikov, Phys. Lett. B **513**, 119 (2001).
[38] P. Fayet, Phys. Rev. D **75**, 115017 (2007).
[39] M. Pospelov, Phys. Rev. D **80**, 095002 (2009).

[40] B. Holdom, Phys. Lett. **166B**, 196 (1986).
[41] For a convenient reference, see Ref. [42] and references therein.
[42] H. S. Lee and S. Yun, Phys. Rev. D **93**, 115028 (2016).
[43] H. Davoudiasl, H. S. Lee, and W. J. Marciano, Phys. Rev. D **85**, 115019 (2012).
[44] H. S. Lee and M. Sher, Phys. Rev. D **87**, 115009 (2013).
[45] H. Davoudiasl, W. J. Marciano, R. Ramos, and M. Sher, Phys. Rev. D **89**, 115008 (2014).
[46] K. Kong, H. S. Lee, and M. Park, Phys. Rev. D **89**, 074007 (2014).
[47] D. Kim, H. S. Lee, and M. Park, J. High Energy Phys. 03 (2015) 134.
[48] L. J. Hall, K. Jedamzik, J. March-Russell, and S. M. West, J. High Energy Phys. 03 (2010) 080.
[49] J. Baur, N. Palanque-Delabrouille, C. Yèche, C. Magneville, and M. Viel, J. Cosmol. Astropart. Phys. 08 (2016) 012.
[50] E. Masso, F. Rota, and G. Zsembinszki, Phys. Rev. D **66**, 023004 (2002).
[51] P. Graf and F. D. Steffen, Phys. Rev. D **83**, 075011 (2011).
[52] A. Salvio, A. Strumia, and W. Xue, J. Cosmol. Astropart. Phys. 01 (2014) 011.
[53] M. Bolz, A. Brandenburg, and W. Buchmuller, Nucl. Phys. **B606**, 518 (2001); **B790**, 336(E) (2008).
[54] M. Fukugita, S. Watamura, and M. Yoshimura, Phys. Rev. Lett. **48**, 1522 (1982).
[55] P. Arias, D. Cadamuro, M. Goodsell, J. Jaeckel, J. Redondo, and A. Ringwald, J. Cosmol. Astropart. Phys. 06 (2012) 013.
[56] A. Pilaftsis and T. E. J. Underwood, Nucl. Phys. **B692**, 303 (2004).
[57] M. Kawasaki, K. Kohri, and T. Moroi, Phys. Rev. D **71**, 083502 (2005).
[58] R. Essig, E. Kuflik, S. D. McDermott, T. Volansky, and K. M. Zurek, J. High Energy Phys. 11 (2013) 193.
[59] A. Boyarsky, J. Lesgourgues, O. Ruchayskiy, and M. Viel, Phys. Rev. Lett. **102**, 201304 (2009).
[60] A. Harada and A. Kamada, J. Cosmol. Astropart. Phys. 01 (2016) 031.
[61] A. Kamada, K. T. Inoue, and T. Takahashi, Phys. Rev. D **94**, 023522 (2016).
[62] S. V. Demidov and D. S. Gorbunov, Phys. Rev. D **90**, 035014 (2014).
[63] S. J. Asztalos *et al.* (ADMX Collaboration), Phys. Rev. Lett. **104**, 041301 (2010).
[64] Y. K. Semertzidis, CAPP: Axions and proton EDM, *Light Dark World International Forum, Daejeon, Korea* (2016).
[65] A. Wagner *et al.* (ADMX Collaboration), Phys. Rev. Lett. **105**, 171801 (2010).
[66] J. Jaeckel and M. Spannowsky, Phys. Lett. B **753**, 482 (2016).
[67] A. Alves, A. G. Dias, and K. Sinha, J. High Energy Phys. 08 (2016) 060.